# RESULTS of the CESR UPGRADE

D.L.Rubin *
Laboratory of Nuclear Studies, Cornell University, Ithaca, NY 14853, USA

## 1 INTRODUCTION

In 1994, the optics of the CESR electron-positron collider were reconfigured for operation with trains of closely space bunches. In the Spring of 1998 the number of bunches in each of the nine trains was increased from two to three. With the installation of the superconducting final focus quadrupoles in 1999, CESR will operate with nine five-bunch trains in each beam.

The higher beam current will be supported by single-cell superconducting RF cavities. The four cavities will support a total beam current of 1A. And with an accelerating gradient 10MV/m the bunch length in CESR will be reduced to 13mm. Because of the very low impedance of the superconducting RF, we anticipate the longitudinal instability threshold to be in excess of 1A. The first superconducting cavity has been in operation in CESR since October of 1997.

The remaining 3 RF cavities will be installed as they are assembled during the next year. The interaction region optics will be replaced in 1999 with a hybrid of permanent magnet quadrupole and superconducting quadrupoles so that the vertical $\beta$ at the IP can be reduced from 18mm to 13mm.

In the Spring of 1998 CESR operated with 27 bunches and 200mA in each beam at the start of fills for high energy physics. We measured a peak luminosity of $5.6 \times 10^{32} cm^{-2} s^{-1}$ corresponding to a beam-beam tune shift parameter of about 0.044.

## 2 BUNCH TRAINS AND CROSSING ANGLE

In CESR the counterrotating beams share a common vacuum chamber. Electrostatic separators are used to differentially displace the orbits of the electron and positron beams so that there are collisions only at the single interaction point inside of the experimental detector CLEO. The beam trajectories intersect at the interaction point with a small horizontal crossing angle. The crossing angle serves to horizontally separate the beams at the nearby parasitic crossing points. The 'pretzeled' orbits are indicated in Figure 1. Note the two parasitic crossing points on either side of the IP that arise with three bunches in each train.

The length of each train is limited by the pretzel scenario to be about 60% of a betatron half wavelength. The minimum spacing of bunches within the train is determined by the effective transverse separation of the bunches at the parasitic crossing nearest the interaction point. Near the

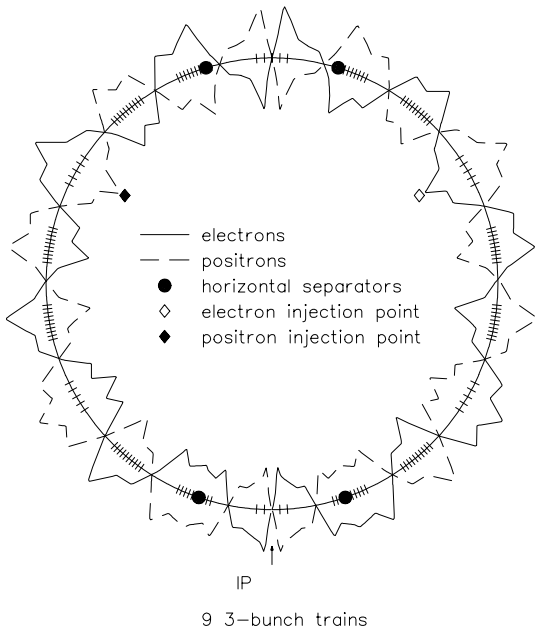


Figure 1: Pretzeled orbits. The maximum horizontal displacement of the beams from the center of the vacuum chamber is about 20mm. The tic marks indicate the parasitic crossing points of electron and positron bunches corresponding to 9 trains with 3 bunches/train. The bunches within each train are temporally separated by 28ns.

interaction point the long range beam-beam tune shift

$$\Delta Q_{h,v} = r_0 N \frac{\beta_{h,v}}{2\pi\gamma(2\theta_c^* \sin\phi_h \sqrt{\beta_h^* \beta_h})^2},$$

where $\theta_c^*$ is the crossing half angle and $\phi_h$, $\beta_h$, and $\beta_v$ the horizontal betatron phase advance and horizontal and vertical $\beta$-function at the parasitic crossing point. If the bunches within each train are spaced 28ns apart, the first parasitic crossing is 4.2m from the IP. With 10mA/bunch the long range horizontal tune shift due to that single interaction is small, $\Delta Q_h \sim 3 \times 10^{-4}$. The vertical tune shift is about half the horizontal and there is negligible effect on specific luminosity. But if the bunch spacing is reduced to 14ns, then the first parasitic interaction is 2.1m from the IP and the vertical long range tune shift increases by an order of magnitude. We find that the specific luminosity is degraded and injection efficiency is compromised. In order to accomodate the more closely spaced bunches the interaction region optics will be modified to reduce the $\beta$-functions at that 2.1m crossing point. Schematics of the interaction region optics are shown in Figure 2. The existing configuration is designated Phase II and the upgraded configuration Phase III. Note that at 2.1m from the IP the value of $\beta$ in

* Work supported by the National Science Foundation

the Phase III interaction region is less than 40m, which is typical of the amplitude of the $\beta$-function throughout the machine arcs.

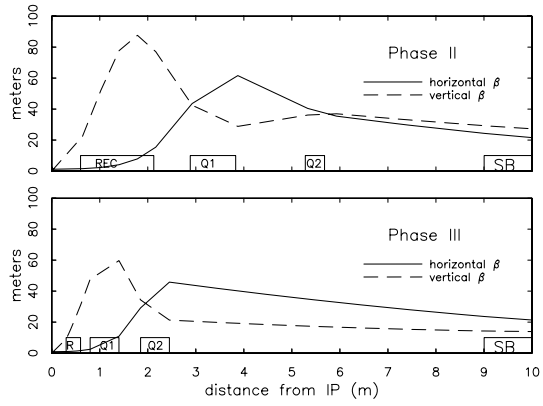


Figure 2: Upper plot shows optical functions in Phase II IR based on 1.5m long permanent magnet quadrupole(REC). With installation of superconducting quadrupoles (Q1 and Q2) in Phase III, $\beta_v^* \sim 10mm$ and $\beta_v$ at the parasitic crossing 2.1m from the IP is $30m$.

## 3 LONG RANGE BEAM-BEAM EFFECTS

In a single turn each bunch of electrons has a close enounter with all 27 bunches of positrons (3 cars in each of 9 trains). The result of the close encounters is that the closed orbit and optical functions of the electron beam depends on the current in the positron beam. Furthermore, the displacements and $\beta$-function at parasitic crossings experienced by cars at the ends of the trains are different than for cars in the middle of the train. Therefore the optical functions of an electron bunch depend on its location in the train. The lower plot in Figure 3 indicates the betatron tune of a single bunch in one beam as a function of the current in each of 27 bunches in the opposing beam. The effect of the collision at the interaction point is excluded. The upper plot in Figure 3 shows the tune of each of the bunches in one beam with fixed current in the opposing beam. The bunch to bunch variation is small compared to the fundamental beam-beam tune shift.

## 4 INJECTION

The effect of the multiple parasitic long range interactions is perhaps most evident during the injection process. At the conclusion of a luminosity run, the remaining electrons are extracted and then the positron beam is topped off. About $10^4$ cycles of the linac-synchrotron injector are required to refill the positrons. Then the horizontal electrostatic separators are powered so that the electron and positrons bunches will be horizontally separated at the interaction point as well as at all of the parasitic crossing points. Injection is into the horizontal phase space so that

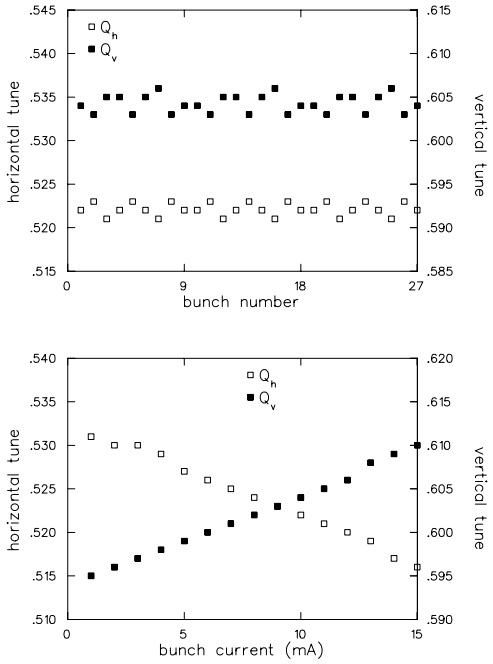


Figure 3: Upper plot indicates betatron tune of each of the bunches in one beam with fixed current of 10mA/bunch in the opposing beam. The lower plot shows the dependence of the tune in the bunches in one beam on the current in the opposing beam.

the injected bunch executes horizontal betatron oscillations about the closed orbit of the electrons. The oscillation amplitude decays with the characteristic radiation damping time of about 10,000 turns. During the first several hundred turns, an injected bunch will experience many very near encounters with the counterrotating stored positrons. Electrons that approach the core of the positron beam are subjected to a strong vertical focusing force[1]. The phase space density and focal strength of the positron beam is reduced by operating with the tunes of the positron beam near the coupling resonance, and introducing skew quadrupoles into the lattice.

Because the horizontal closed orbits of electron and positron beams are different, the tunes of the two beams can be set independently by manipulating the sextupole distribution. We define tonality as the difference in tunes. As noted above, the positrons are tuned to the coupling resonance. The horizontal tune of the electron beam is set well below the horizontal tune of the positron beam, limiting the transverse coupling of the electrons. Electron injection is most efficient if the electron and positron horizontal tunes are very different, (large horizontal tonality). Presumably the tune difference decouples the betatron motion of the two beams.

## 5 LONGITUDINAL INSTABILITY

A longitudinal coupled bunch instability is excited by high Q parasitic modes in the normal conducting RF acceler-

ating cavities. The instability threshold depends in detail on the number and distribution of bunches in the beam. The threshold is sensitive to the temperature of the RF cavities and therefore to the frequency of the higher order modes[2]. In addition, a longitudinal coupled bunch mode is excited by interaction of the beam with the cavity fundamental[3]. With the replacement of the room temperature 5-cell cavities with single cell superconducting cavities, the total impedance at the fundamental will decrease by a factor of fifteen and all of the high Q parasitic modes will be eliminated. We anticipate that the longitudinal instability threshold will be well in excess of the 1A design current.

A longitudinal feedback system has been implemented so that we can continue to increase total beam current while the remaining superconducting RF cavities are being assembled. The system consists of a receiver, a digital filter processor, power amplifier, and kicker. The receiver is essentially a phase detector. The signal from a beam position monitor is mixed with the CESR RF reference. The amplified output is proportional to the arrival time of the bunch.

The signal processor operates at the maximum bunch frequency of 71MHz (minimum spacing of 14ns), with an in line pedestal correction[4]. A two pole low pass filter eliminates spurious high frequencies including the betatron frequencies, from the digitized signal. The low pass filter is followed by a tuneable band pass filter. Both filters are infinite input filters fabricated with programable array logic.

A horizontal stripline kicker couples to the longitudinal motion of the beam. There is finite dispersion in the lattice at the location of the kicker. A differential pulse on the two plates of the stripline generates a horizontal kick that drives the beam longitudinally by modulating the path length of the beam. A common pulse on the two plates couples to the beam energy via the voltage developed across the gap at the end of the kicker plates.

During the past year a broadband analog power amplifier was used to drive the kicker differentially. In the next few months the analog amplifier will be replaced by a fixed amplitude pulser[5]. The pulser will drive the stripline in the acceleration mode to minimize coupling to the betatron motion. At each bunch passage, the modulator sends an 1100V pulse to the kicker if the digitized error signal is greater than a random number. The sign of the kick for the fixed pulse can be reversed by advancing the pulse so that the bunch passage is coincident with its reflection.

The instability excited by the cavity fundamental corresponds to a single multi-bunch mode at the synchrotron sideband below the first revolution harmonic. The phase of the RF cavity drive is modulated at the frequency of the sideband to damp the instability.

## 6 SUPERCONDUCTING RF

A single cell, superconducting RF cavity system has been developed to support the high current multiple bunch beams in CESR[6]. The accelerating mode resonates at 500MHz. The impedance in the fundamental of the single cell cavity is 1/15 of the 5-cell copper cavity that it replaces. Due to the open geometry of the cell and large beam tube, the R/Q of the higher order modes is small. Furthermore, all of the higher order modes propagate along the 24cm diameter beam tube to ferrite absorbers that line that same beam tube outside the cryostat. The Q values of higher order modes are less than $\sim 100$.

RF power is transmitted into the cavity through a waveguide input coupler and a planar ceramic waveguide window. The cavities are designed to operate at a gradient of 10MV/m while transmitting 325kW to the beam. Four cavities will support a 1A beam with a bunch length of 13mm.

The first superconducting cavity was installed in CESR in October 1997. The accelerating voltage was set to 1.9MV to match the copper cavity that it replaced. With pulse processing and CW operation with beam, the power that could be transmitted to the beam through the cavity increased to 140kW. Continued processing was ineffective at raising that limit. The cavity was then warmed to room temperature, the window was baked, and condensates on the window and waveguide coupler were pumped out. Subsequently, 180kW could be transmitted to the beam. The total transmitted power was limited only by the room temperature cavity with which the superconducting cavity shares a single klystron. The processing history is shown in Figure 4. The superconducting cavity has suppported a CESR record total beam current of 450mA.

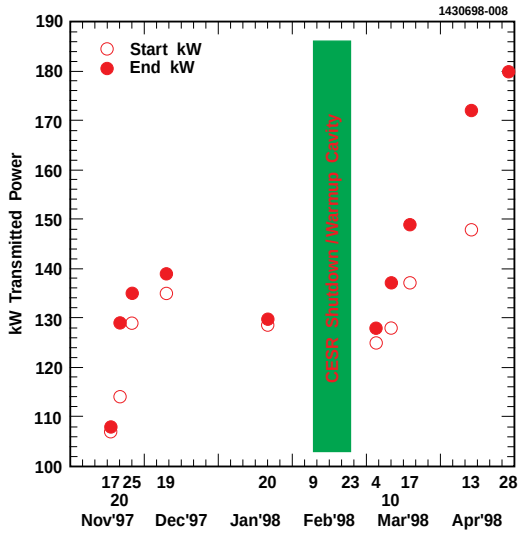


Figure 4: Window/coupler processing history of superconducting RF cavity. The open and closed circles correspond to the start and end of pulse processing. The shaded region in February indicates cavity warmup.

The second superconducting cavity will be installed in October 1998 and the remaining two cavities in the Spring of 1999.

## 7 CURRENT LIMITS

During the past few years the current limiting phenomona have included overheated vacuum components, longitudinal instability, cavity and window arcs, separator photocurrents, and losses associated with bringing beams into collision. Our goal is that the storage ring support a total beam current of 1A. Many vacuum chamber components have been modified for better cooling or masked from offending synchrotron radiation. The longitudinal instability is now effectively damped by feedback. Both superconducting and room temperature RF cavities have responded successfully to beam processing.

There are at least two distinct sources of photocurrent in the electrostatic separators. Photoelectrons are produced where direct synchrotron radiation strikes the copper absorbers. Current develops between the absorber and the positive separator plate. Permanent magnets are placed around the absorbers to trap photoelectrons, significantly reducing the current from ground potential to positive plate.

Indirect photons that have scattered at least once in the adjacent vacuum chambers strike the negative plate. The resulting photocurrent flows between the plates and appears as an equal current on the positive and negative power supplies. In an attempt to reduce the intensity of indirect photons, the neighboring vacuum chamber has been modified with shallow steps so that single scattered photons cannot reach the negative plates. The high voltage power supply, which had limited at 5.7mA has been replaced with a 16mA device. The modified chamber and higher current supply were installed within the last few weeks.

The transition from injection conditions, where the beams are separated at the interaction point, to colliding beams, involves changes in orbits, tunes, tonalities and chromaticity. Because of the current dependent distortion of orbits and optical functions of one beam on the other described above, each incremental increase in beam current that we bring to collision requires modification of the operating point. We find the higher current operating point empirically.

## 8 LUMINOSITY

Beam-beam performance depends critically on transverse coupling and solenoid compensation, tonality, the sextupole distribution and the vertical orbit. The sextupole distribution is designed to minimize the amplitude and energy dependence of the optical functions and to maximize the effective linear aperture. Control algorithms are implemented that permit variations in chromaticity and tonality that preserve the other features of the distribution. In general we find that the maximum beam-beam tune shift is achieved at the minimum chromaticity consistent with good beam lifetime, typically a few units less than zero.

As has been observed at other electron positron colliders, beam-beam performance at CESR depends on the details of the vertical orbit[7]. The sensitivity to vertical orbit is presumably related to the transverse coupling of a beam that is off axis in sextupoles, the vertical dispersion generated in a beam that is displaced in quadrupoles, and perhaps nonlinearity of the vertical correctors themselves. The phenomona are not well understood and the orbit is tuned empirically to maximize luminosity.

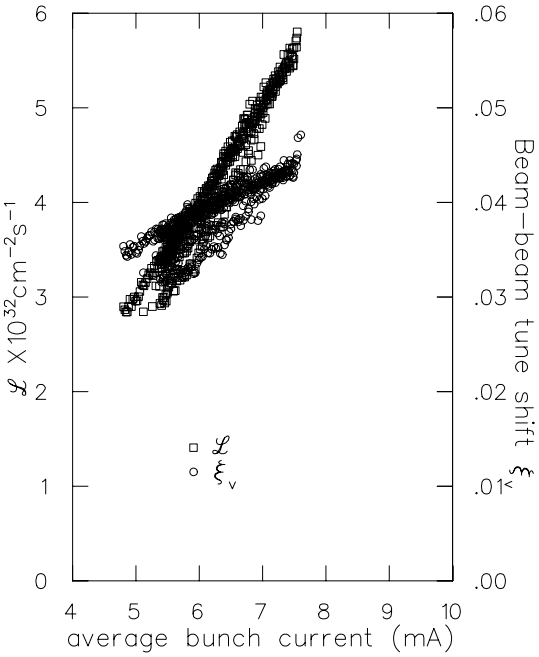


Figure 5: Luminosity and beam-beam tune shift parameter vs bunch current.

Beam-beam coupling is monitored by vertically shaking one beam at a frequency far from the machine tunes, and measuring the response of the opposing beam at the shaker frequency with a lock-in amplifier[8]. With appropriate gating we measure the beam-beam coupling, which is proportional to the luminosity, for each pair of colliding bunches independently. We find that the vertical orbits of the bunches are not identical, and that the luminosity is optimized for each bunch in the train with a slightly different vertical orbit. The effect is thought to be due to wakefields.

The current dependence of luminosity and beam-beam tune shift parameter is shown in Figure 5. The peak luminosity, and daily integrated luminosity have continued to rise with increasing beam current and beam-beam tune shift parameter. The parameters describing the CESR configuration (CESR Phase II) and performance in the Spring of 1998 are summarized in Table 1. For the 1997 calender year CESR integrated $3400pb^{-1}$ and to date $1851pb-1$ in 1998. Our most recent full month of operation, April, 1998 was also our best and we accumulated $498pb^{-1}$. The maximum total beam current brought to collision is 435mA. The monthly integrated luminosity history is shown in Figure 6.

## 9 PHASE III

Phase III of the CESR luminosity upgrade involves replacement of the final focus quadrupoles and interaction region

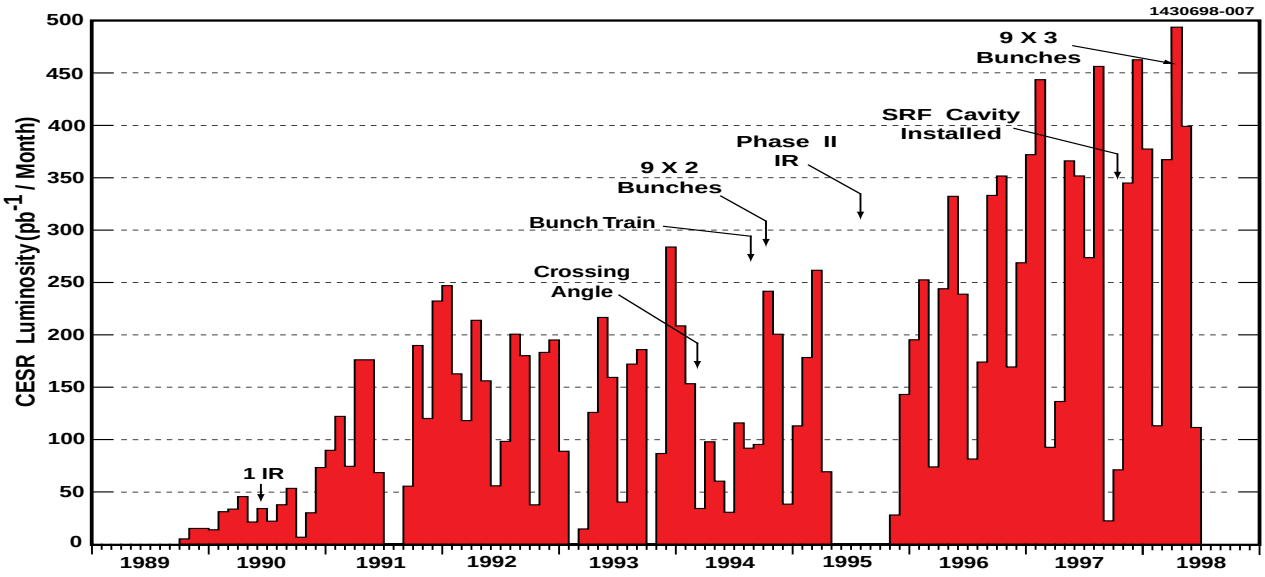


Figure 6: Integrated luminosity per month.

vacuum chambers and is scheduled to coincide with the installation of the CLEO III detector in the Spring of 1999. A layout of the quadrupoles is shown in the lower plot in Figure 2. The first of the three quadrupoles is a 28cm long neodymium iron boron permanent magnet with front end 33cm from the interaction point. The vertically focusing magnet is assembled from three 9.3cm long sections. The gradient of the first section is 29.27T/m and the gradient of the remaining two sections is 31.91T/m.

The magnets labeled Q1 and Q2 in the lower plot in Figure 2 are vertically and horizontally focusing superconducting magnets that share a common cryostat. The length of each of the magnets is 62cm. Each magnet consists of a superposition of quadrupole coils, skew quad coils and vertical dipole corrector windings. The design gradient of the quadrupole is 48T/m. With the Phase III interaction region quadrupoles, $\beta_v$ at the IP can be reduced to as low as 10mm and as noted above, bunches spaced as few as 14ns apart by virtue of moderate values of $\beta$ at the 2.1m parasitic crossing.

Q1 is entirely and Q2 partially inside the 1.5T field of the CLEO solenoid. The transverse coupling generated by the solenoid is compensated roughly by rotating the entire superconducting magnet assembly $4.5^\circ$ about the beam axis and then precisely with the superposed skew quad windings.

The CESR Phase III design parameters are summarized in Table 1. With completion of the installation of the superconducting RF cavities and the upgrade of the interaction region optics, CESR will have the capability to store 500mA/beam in nine 5-bunch trains. The practical minimum $\beta_v^*$ will be limited by the natural bunch length to 13mm. At a beam-beam tune shift parameter of $\xi_v \sim 0.04$, we anticipate peak luminosity $\sim 1.7 \times 10^{33}\,\mathrm{cm}^{-2}\mathrm{s}^{-1}$.

Table 1: CESR Parameters

| | Today (Phase II) | Phase III |
|---|---|---|
| beam energy[GeV] | 5.289 | 5.289 |
| 5-cell copper cavities | 3 | 0 |
| single cell SRF cavities | 1 | 4 |
| RF accelerating voltage[MV] | 6.4 | 12 |
| $\beta_v^*$[mm] | 18 | 13 |
| $\beta_h$ 2.1m from IP [m] | 14 | 29 |
| $\beta_v$ 2.1m from IP [m] | 78 | 30 |
| natural bunch length[mm] | 19 | 13 |
| number of bunch trains | 9 | 9 |
| number of bunches/train | 3 | 5 |
| bunch spacing [ns] | 28 | 14 |
| peak colliding beam current [A] | 0.406 | 1 |
| crossing angle [mrad] | 2.1 | 2.7 |
| vert tune shift param | 0.044 | 0.04 |
| luminosity[$\times 10^{32} cm^{-2} s^{-1}$] | 5.6 | 17 |

## 10 REFERENCES


[1] Temnykh,S. and Pozdeev,E., CBN 98-3, January 1998.

[2] Billing,M., Proceedings of the 1997 PAC, Vancouver.

[3] Fromowitz,D., CON 97-10, August 1997.

[4] Meller,R.E., private communication, 1998.

[5] Codner,G. Proceedings of Beam Instrumentation Workshop, Stanford, CA, May 1998.

[6] Belomestnykh, S. et. al., Proceedings 1997 PAC, Vancouver.

[7] Hylas, J. private communication

[8] Sagan,D.,Sikora,J., and Henderson,S., CBN 97-13, 1997.